ALIASING IN INFORMATION PROCESSING AND INTERPOLATING RANDOM SIGNALS BY CUBIC SPLINE

N. FAGHIH, Ph. D.
Shiraz University, Shiraz, I. R. of Iran
email: nfaghih@rose.shirazu.ac.ir

Abstract - This paper considers the problem of aliasing in information processing. The cubic spline method of interpolating the uniformly sampled signals and its effects on the autocorrelation estimation as well as the resulting spectral density function are studied by simulating random signals with known autocorrelation functions. Hence, by comparison of aliased and alias-free cases, indications are deduced from suspection to aliasing, especially in those situations that aliasing is present but the Nyquist frequency is not too far apart from the main peaks in the signal.

Keywords - Aliasing, Information Processing, Cubic Spline, Interpolation, Random Signals, Autocorrelation Function, Spectral Density, Time Series.

INTRODUCTION

Aliasing is a major problem arising in the digital processing of time series, especially when using the conventional method of uniform sampling. It is a well-known problem, a detailed account of which may, for instance, be found in [1-2], and yet a considerable issue encountered in spectral analysis [3-8]. The cubic spline method of interpolation, well established in numerical analysis [9], has also been recently applied to a variety of problems in signal analysis [10-14].

Therefore, by simulating signals, the cubic spline method is applied to interpolate the autocorrelation function and random signal. This allows to investigate the effect of cubic spline interpolation on the resulting spectral density function.

Consider the equi-spaced discrete signal with a sampling time interval $\Delta\tau$. From these discrete data, a discrete autocorrelation function $R(\tau)$, with an equi-spaced interval $\Delta\tau$, is obtainable. The autocorrelation function and also the dirac delta function, $\delta(\tau)$, are both even functions and hence the discrete autocorrelation function, $R^*(\tau)$, may be represented as [1]:

$$R^*(\tau) = \Delta\tau \, . R(\tau) \delta_c(\tau) \qquad (1)$$

where,

$$\delta_c(\tau) = \sum_{n=0}^{\infty} \delta(\tau - n\Delta\tau) \qquad (2)$$

The Fourier transformation of $R^*(\tau)$ gives the spectral density corresponding to the sampled signal and that of $R(\tau)$ yields the spectral density of the original continuous

signal. Let the formcr be denoted by $S^*(\omega)$ and the latter by $S(\omega)$, where $\omega = 2\pi f$ for the frequency f. Fourier transformation of equation (1) can be shown [1] to give:

$$S^*(\omega) = \sum_{-\infty}^{\infty} S(\omega + 2n\omega_c), \omega_c = \pi / \Delta\tau \qquad (3)$$

Equation (3) suggests that $S^*(\omega)$ is periodic, with period $2\omega_c$. This fact can also be shown by employing the properties of discrete Fourier transformation [1-2]; i.e., for any integer m:

$$S^*(\omega + 2m\omega_c) = S^*(\omega) \qquad (4)$$

which is the mathematical statement for $S^*(\omega)$ to be periodic with period $2\omega_c$.

Although $S^*(\omega)$ has a period of $2\omega_c$ when only positive frequencies are considered, its fundamental domain will have a width of ω_c. This indicates that, in the half plane (positive frequency), thc spectrum will be repeated at frequencies beyond ω_c. Since the spectral density is an even function [2], the picture appearing between $\omega=\omega_c$ and $\omega=2\omega_c$ is expected to be the mirror image of that appearing between $\omega=0$ and $\omega=\omega_c$. The samc sequence will, then, be repeated with a period of $2\omega_c$.

The frequency $\omega_c=\pi/\Delta\tau$ (or $f_c=1/2\Delta\tau$) is called the Nyquist, folding or cut-off frequency [1-2]. It should be noted that, due to the periodicity property, no information about the frequency content of the signal, above the cut-off frequency, is obtainable. For the spectral estimation below the cut-off frequency, however, equation (3) must be examined. This equation shows the relationship between thc spectrum corresponding to the sampled signal and that corresponding to the original continuous signal.

It indicates that the spectral densities at frequencies $2n\omega_c \pm \omega$ (or $2nf_c \pm f$) would add to those at ω (or f); these frequencies are called 'aliases'. Therefore, if the sampling interval $\Delta\tau$ is such that frequencies higher than $1/_{2\Delta\tau}$ are present in the original signal, then these will contribute to the useful range $(0, f_c)$; they will be folded back and appear as low frequencies, which can cause confusion over the true frequency content of the signal. The phenomenon is referred to as 'aliasing'. On the other hand, if $\Delta\tau$ is sufficiently small to have $S(\omega+2n\omega_c)=0$ for $n\neq0$, then $S^*(\omega)=S(\omega)$ and the resulting spectrum will be alias-free [1-2].

Not only as an illustration, but also as a later requirement for comparison with the cubic spline interpolation results, the Nyquist frequency and aliasing will be demonstrated by computer simulation of an autocorrelation function. The discrete autocorrelation function was used with different values of $\Delta\tau$ to obtain cut-off frequencies below and above the positions of the main peaks in thc original data. The trapezoidal integration rule, given in [2], was used for Fourier transformation of the discrete autocorrelation functions. The true spectrum is also shown. This was abtained by Fourier transformation of the continuous autocorrelation functions [2].

Consider the autocorrelation function:

$$R(\tau) = \exp(-\tau)\cos 12\pi\tau \qquad (5)$$

The true spectrum, obtained by Fourier cosine transformation of this funcion, is shown in Figure 1. The spectrum exhibits a peak at f=6.

The discrete autocorrelation function was used with $\Delta\tau=0.025$. This value gives a non-dimensional cut-off frequency $f_c=20$, which is well above the frequency at which

the peak occurred in the true spectrum. The spectral estimates were obtained in the frequency range 0 to $2f_c$, by cosine transformation of the discrete function (sufficient number of lag values were used to allow its decay). This is shown in Figure 2, where it is seen that a peak is exhibited at the frequency of 6, which is in agreement with the true spectrum. The spectrum in the range f_c to $2f_c$ (20 to 40) is, however, seen to be merely the mirror image of that in the range 0 to f_c (0 to 20). Hence, the useful frequency range for spectral estimation is 0 to f_c.

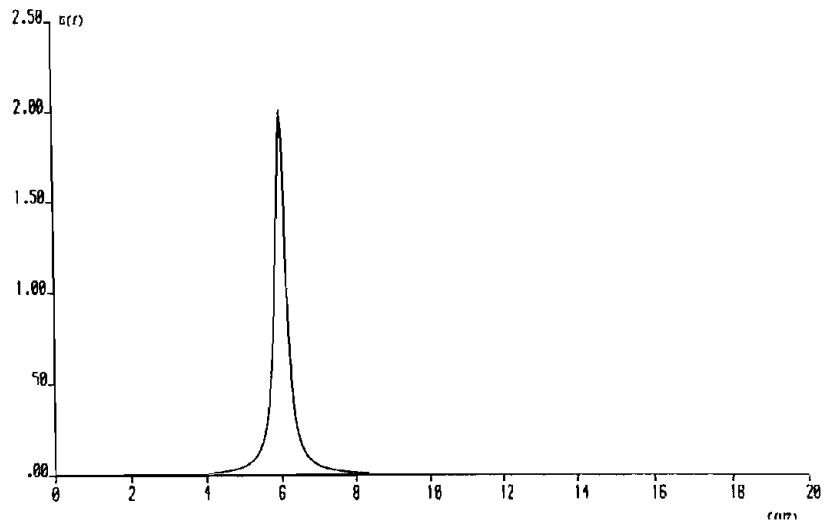

Figure 1: The true spectrum obtained by cosine transformation of the autocorrelation function: $R(_\tau) = \exp(-_\tau) \cos(12_{\pi\tau})$

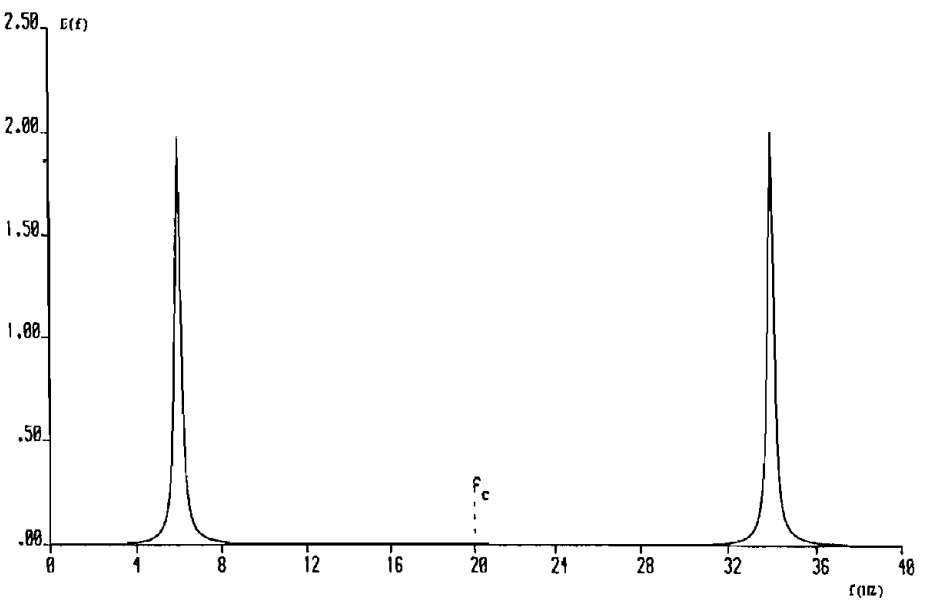

Figure 2: The spectral estimate from the autocorrelation function: $R(_\tau) = \exp(-_\tau) \cos(12_{\pi\tau})_{\Delta\tau} = 0.025$s.

A value of $\Delta\tau$=0.1 was, then, used. This gives a cut-off frequency f_c=5, which is less than the present frequency (i.e., 6). Since the frequencies f and $2nf_c \pm f$ are aliases, it is expected that the peak at 6 should contribute to the frequency of 4. The spectral estimates were computed in the range 0 to $2f_c$ (0 to 10). The spectrum is shown in Figure 3; it exhibits a peak at 4 and the spectrum in the range f_c to $2f_c$ is seen to be the mirror image of that in the range 0 to f_c. It is noted that the peak obtained at 4 is false; it demonstrates the aliasing occurring in the useful (Nyquist) frequency range.

THE CUBIC SPLINE INTERPOLATION OF SAMPLED SIGNALS

The cubic spline method of interpolation, outlined in the Appendix, may be found in detail in [9]. This paper considers the cubic spline interpolation of random signal, before the estimation of the autocorrelation function, and its effect on the resulting spectrum.

Some random signals with known autocorrelation functions were simulated on a computer, using the methods given in [15-16]. The cubic spline method was used for mid-interval interpolation of the signal. Time interval was, hence, halved and the sample size doubled. Consequently, the cut-off frequency used for spectral estimation was also doubled.

The data with the new sample size and (uniform) time interval, consisting of the original and interpolated values, were used to obtain a discrete autocorrelation function; the approach outlined in [2] was used for the autocorrelation estimation. To avoid the truncation problem, a sufficient sample size was used to let the estimated autocorrelation function decay to zero. The power spectra were obtained by discrete cosine transformation of the estimated autocorrelation functions [2].

The estimated autocorrelation coefficients are shown and compared with the true curves. The estimated spectra are also compared with the true spectra. The true spectra were computed from the continuous cosine transformation of the true autocorrelation functions, as may be found in [2].

Random data with the autocorrelation function:

$$R(\tau) = \exp(-\tau)\cos 12\pi\tau \qquad (6)$$

were simulated. The sampling interval $\Delta\tau$=0.025 was used to give a cut-off frequency well above the main peak. 30000 sample values were simulated and interpolated at the mid-intervals. The autocorrelation coefficients were, therefore, estimated with $\Delta\tau$=0.0125 and the sample size of 60000. The estimated lag values (up to the autocorrelation lag number 50) are shown and compared with the true curve in Figure 4. The estimated values are seen to lie on the true curve and form a good representation of it. The lag values R(0)→R(800) were used to estimate the spectral density function. The spectrum obtained from the estimated function is shown and compared with the true spectrum in Figure 5, where the estimated spectrum is seen to be exact. It is also noted that the spectrum has a cut-off frequency of 40 ($\Delta\tau$=0.0125), which is twice the original cut-off frequency that would have been 20 ($\Delta\tau$=0.025) before interpolation.

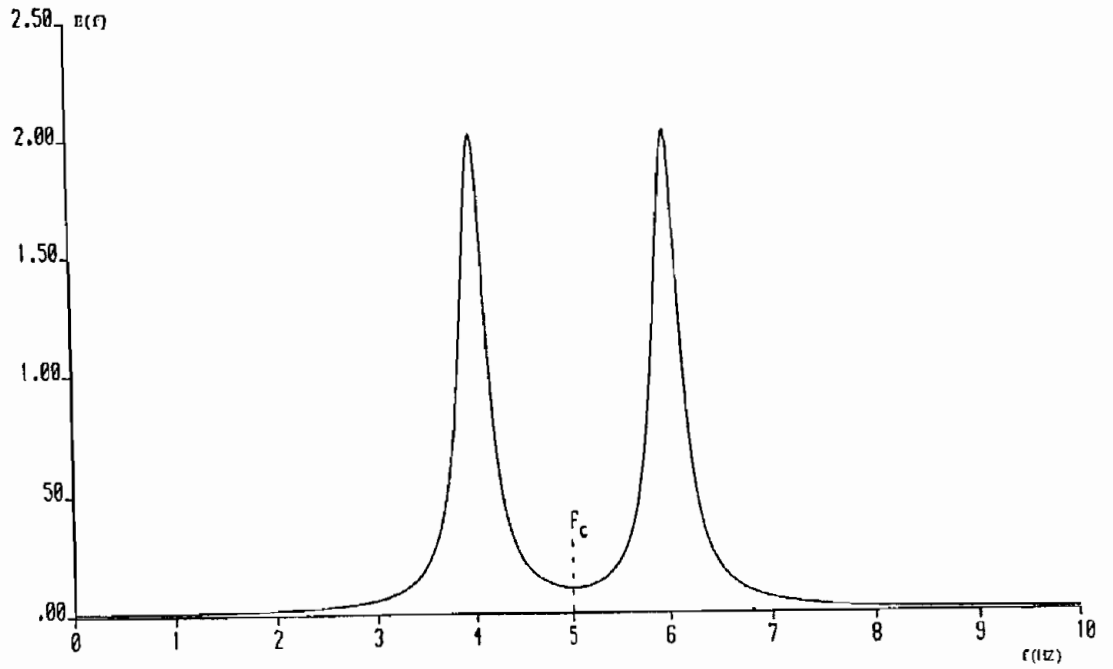

Figure 3: The spectral estimate from the autocorrelation function:
$R(_\tau) = \exp(-_\tau) \cos(12_{\pi\,\tau})_{\Delta\tau}$= 0.1s.

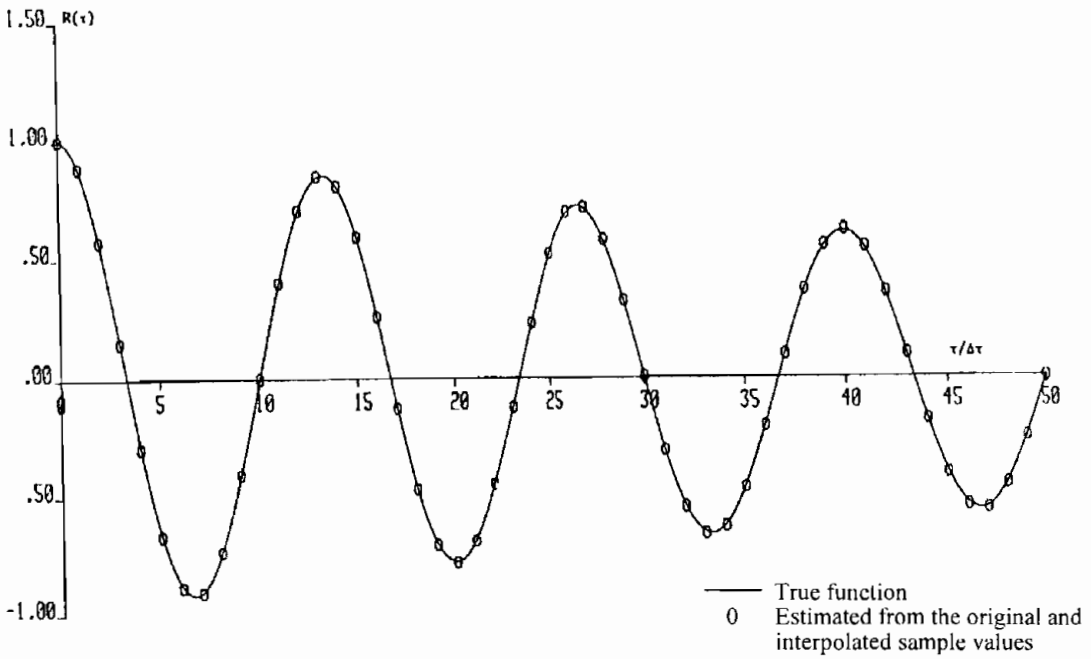

Figure 4: The random data with autocorrelation function:
$R(_\tau) = \exp(-_\tau) \cos(12_{\pi\,\tau})$
The original sample size: 30000 The original time interval: $\Delta\tau = 0.025$s
The new sample size: 60000 The new time interval: $\Delta\tau = 0.0125$s

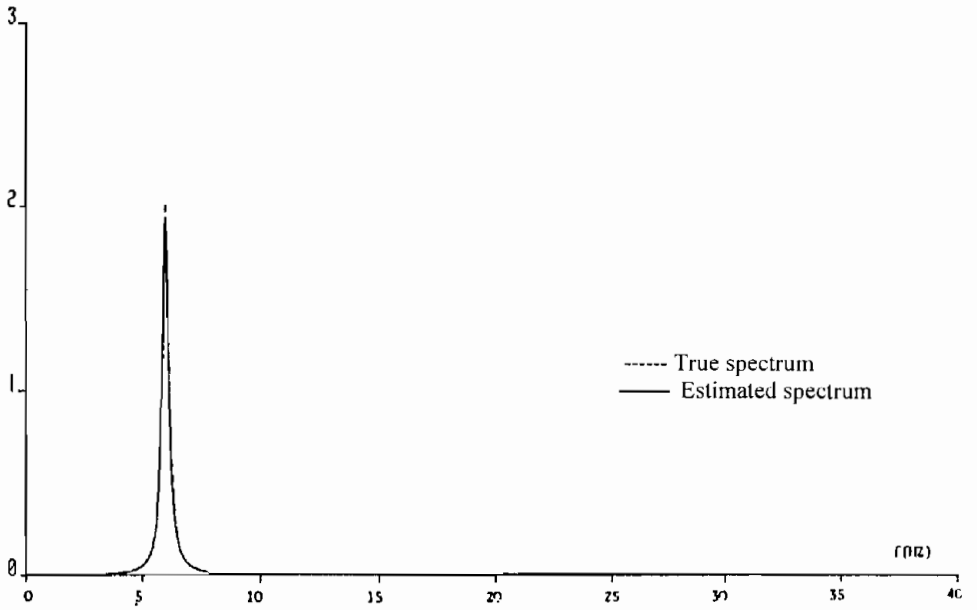

Figure 5: The true spectrum and that obtained by cubic spline interpolation of the data.
The random data with autocorrelation function:
$R(\tau) = \exp(-\tau) \cos(12\pi\tau)$
The cubic spline method applied to mid-interval interpolation of the data
R(0) – R(16) obtained from the original and interpolated values
R(17) – R(800) extrapolated
The original sample size: 30000 The new sample size: 60000
The original cut-off frequency: 20HZ ($\Delta\tau$ = 0.025s)
The new cut-off frequency: 40 HZ ($\Delta\tau$ = 0.0125s)

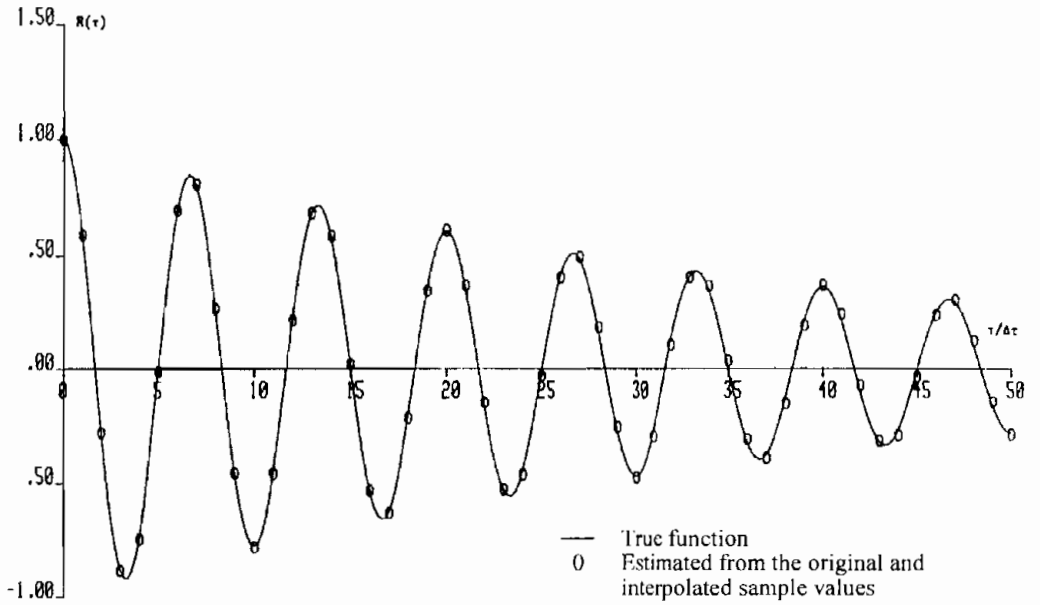

Figure 6: The random data with autocorrelation function:
$R(\tau) = \exp(-\tau) \cos(12\pi\tau)$
The cubic spline method applied to mid-interval interpolation of the data
The original sample size: 30000 The original time interval: $\Delta\tau$ = 0.05s
The new sample size: 60000 The new time interval: $\Delta\tau$ = 0.025s

The value of $\Delta\tau$ was increased to 0.05, which would still give a cut-off frequency above the main peak. The same number of sample values, as before, were simulated and interpolated. Figure 6 shows the autocorrelation coefficients estimated from the original and interpolated values. The estimated lag values are seen to agree with the true function. The estimates of R(0)→R(400) were used (as the decayed autocorrelation function) for spectral estimation. The resulting spectrum is shown in Figure 7, where it is seen to lie on the true spectrum and be a good representation of the latter. The cut-off frequency has also been doubled.

The value of $\Delta\tau$ was further increased to 0.1, which would give a cut-off frequency below the main peak. The data, with the same sample size as before, were simulated and interpolated. The autocorrelation coefficients, estimated from the original and interpolated values, are shown and compared with the true curve in Figure 8. It shows that the estimated lag values, alternately, lie on the true curve, i.e. those with a time delay of 0.1 apart. The estimated coefficients, altogether, appear as a discrete function with a lower frequency than the true function. Nevertheless, some of the values which would not lie on the true curve, fall close to it. At these points, the discrete function becomes approximately close to the true curve. This pattern seems to be repeated periodically. The estimated coefficients R (0)→R(200) were used to estimate the spectrum, which is shown and compared with the true spectrum in Figure 9. The estimated spectrum exhibits a peak at f=4 (which is the alias of 6) and a small peak at f=6, i.e. beyond the original cut-off frequency (i.e., 5).

As an alternative example, random data with the following autocorrelation function were simulated and interpolated:

$$R(\tau) = \exp(-\tau)\cos 10\pi\tau \qquad (7)$$

The same sample size as used for the former data (30000) was employed. The sampling interval $\Delta\tau$=0.025 was used to obtain a cut-off frequency above the main peak. The autocorrelation coefficients, obtained from the original and interpolated data, are shown and compared with the true curve in Figure 10. The lag values R(0)→R(1000) were employed to estimate the spectral density function. The resulting spectrum is shown and compared with the true spectrum in Figure 11. The sampling interval $\Delta\tau$=0.0125, giving a low cut-off frequency, was then used. Figure 12 shows the estimated autocorrelation coefficients and Figure 13 displays the corresponding spectrum. The spectrum was obtained by estimating the autocorrelation function from R(0) to R(200); it is noted that the time delay has been increased and R(200) is sufficient to allow the function to decay.

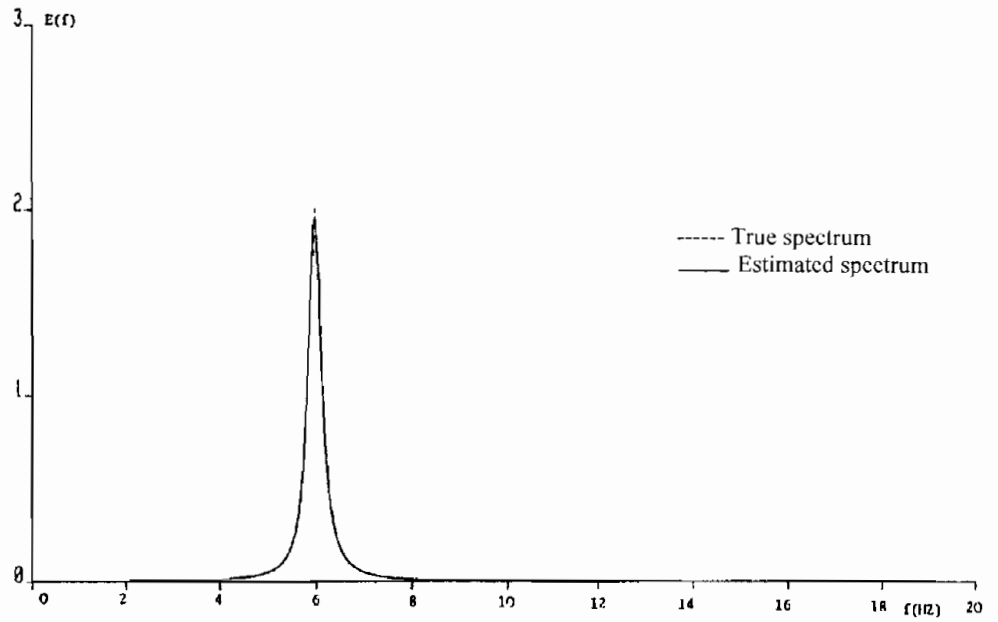

Figure 7: The spectrum and that oblained by cubic spline interpolation of the data.
The random data with autocorrelation function:
$R(_{\tau}) = \exp(-_{\tau}) \cos(12_{\pi\,\tau})$
The cubic spline method applied to mid-interval interpolation of the data
R(0)- R(16) obtained from the original and interpolated values
R(17)- R(400) extrapolated
The original sample size: 30000 The new sample size: 60000
The original cut-off frequency: 10HZ ($\Delta\tau = 0.05$s)
The new cut-off frequency: 20HZ ($\Delta\tau = 0.025$s)

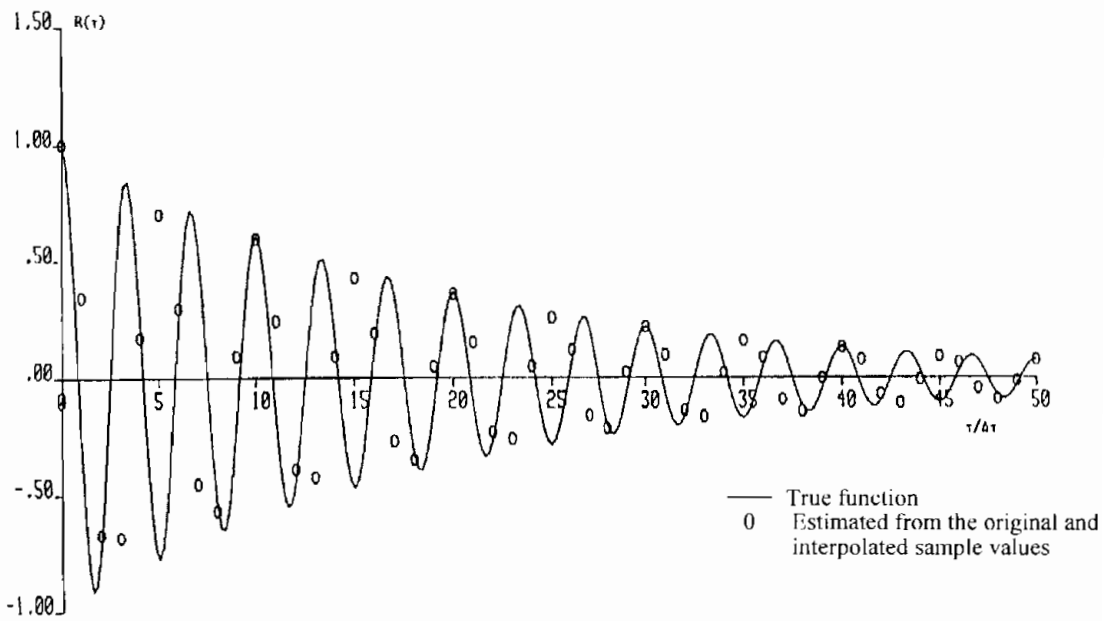

Figure 8: The random data with autocorrelation function:
$R(_{\tau}) = \exp(-_{\tau}) \cos(12_{\pi\,\tau})$
The cubic spline method applied to mid-interval interpolation of the data
The original sample size: 30000 The original time interval: $\Delta\tau = 0.1$s
The new sample size: 60000 The new time interval: $\Delta\tau = 0.05$s

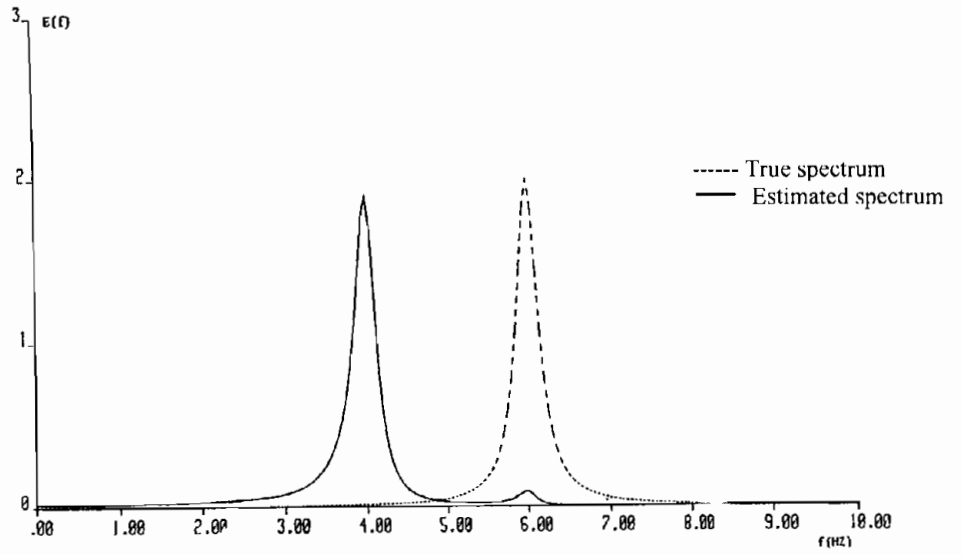

Figure 9: The true spectrum and that obtained by cubic spline interpolation of the data.
The random data with autocorrelation function:
$R(_\tau) = \exp(-_\tau)\cos(12_{\pi\,\tau})$
The cubic spline method applied to mid-interval interpolation of the data
R(0)- R(16) obtained from the original and interpolated values
R(17)- R(200) extrapolated
The original sample size: 30000 The new sample size: 60000
The original cut-off frequency: 5HZ ($\Delta\tau = 0.1$s)
The new cut-off frequency: 10HZ ($\Delta\tau = 0.05$s)

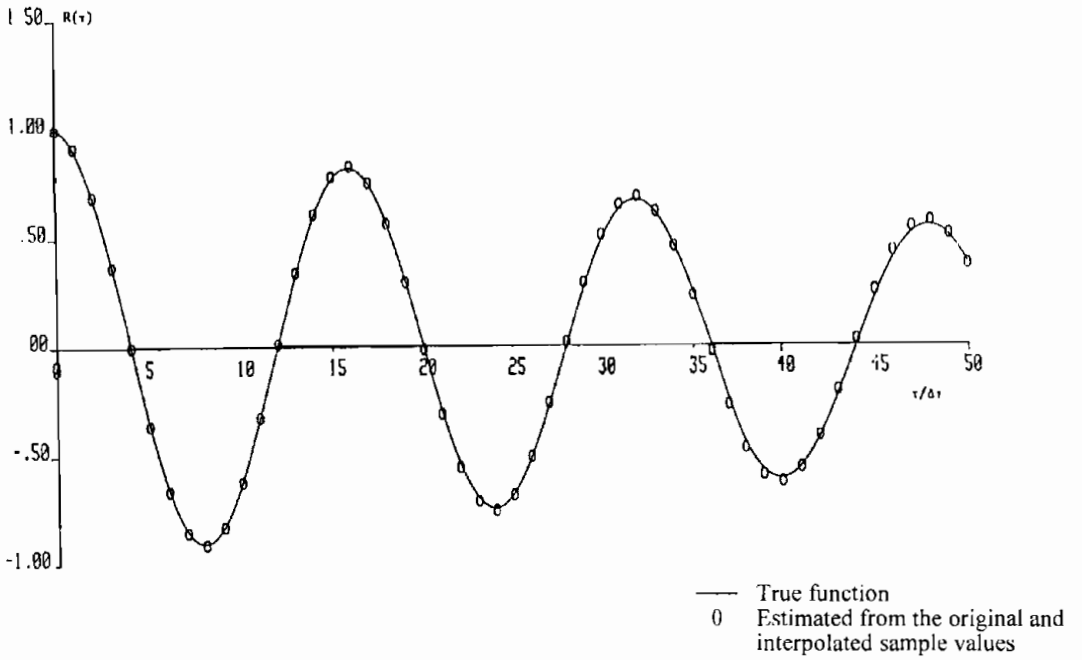

Figure 10: The random data with autocorrelation function:
$R(_\tau) = \exp(-_\tau)\cos(10_{\pi\,\tau})$
The cubic spline method applied to mid-interval interpolation of the data
The original sample size: 30000 The original time interval: $\Delta\tau = 0.025$s
The new sample size: 60000 The new time interval: $\Delta\tau = 0.0125$s

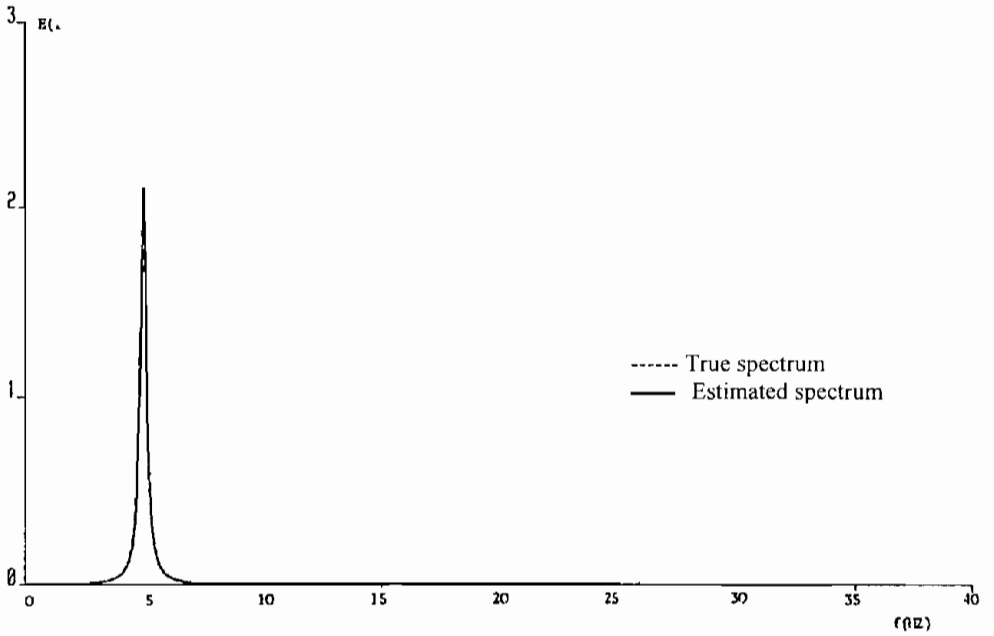

Figure 11: The true spectrum and that obtained by cubic spline interpolation of the data.
The random data with autocorrelation function:
$R(\tau) = \exp(-\tau) \cos(12\pi\tau)$
The cubic spline method applied to mid-interval interpolation of the data
R(0)- R(20) obtained from the original and interpolated values
R(21)- R(200) extrapolated
The original sample size: 30000
The original cut-off frequency: 20HZ ($\Delta\tau = 0.025$s)
The new cut-off frequency: 40HZ ($\Delta\tau = 0.025$s)

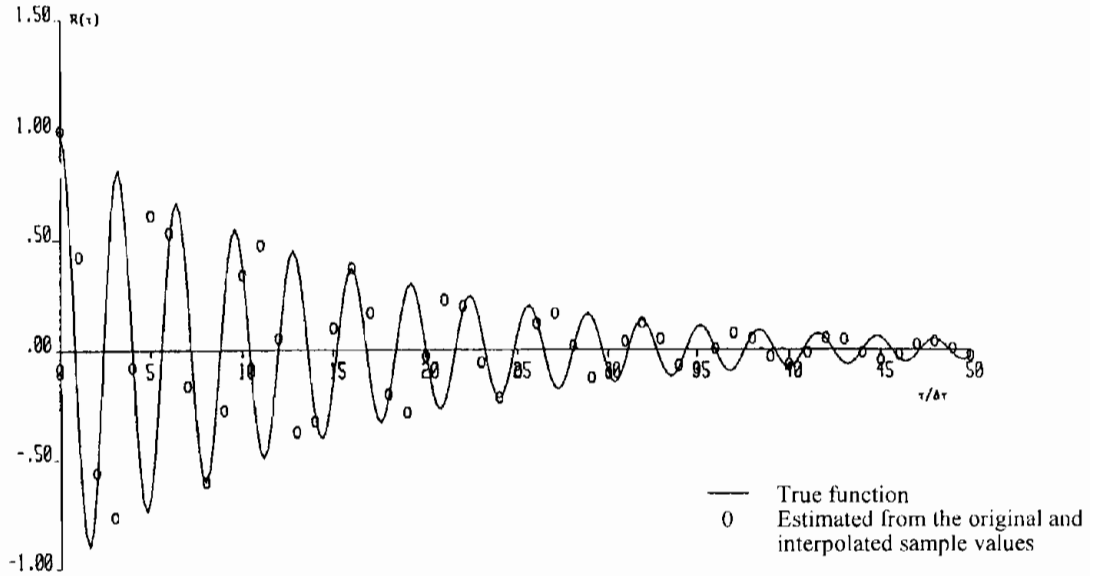

Figure 12: The random data with autocorrelation function:
$R(\tau) = \exp(-\tau) \cos(10\pi\tau)$
The cubic spline method applied to mid-interval interpolation of the data
The original sample size: 30000 The original time interval: $\Delta\tau = 0.125$s
The new sample size: 60000 The new time interval: $\Delta\tau = 0.0625$s

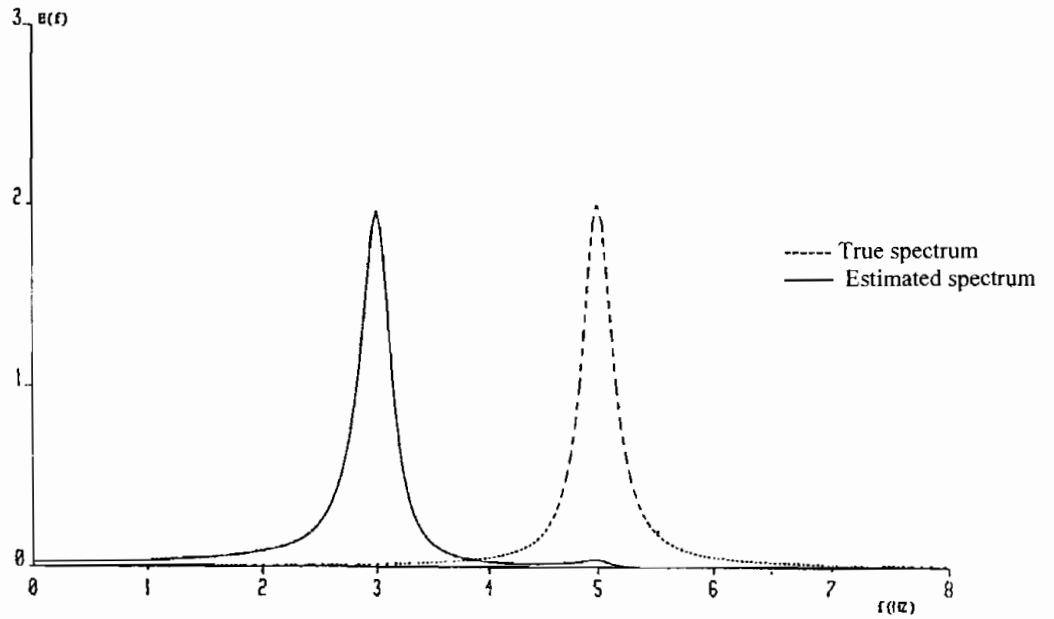

Figure 13: The true spectrum and that abtained by cubic spline interpolation of the data.
The random data with autocorrelation function:
$R(_\tau) = \exp(-_\tau) \cos(10_{\pi\,\tau})$
The cubic spline method applied to mid-interval interpolation of the data
R(0)- R(20) obtained from the original and interpolated values
R(21)- R(200) extrapolated
The original sample size: 30000
The original cut-off frequency: 20HZ ($\Delta\tau = 0.125$s)
The new cut-off frequency: 40HZ ($\Delta\tau = 0.0625$s)

The observations from these figures are similar to the previous data. In the first case (aliased), the estimated lag values lie on the true curve. The spectrum is exact and no peaks are exhibited beyond the original cut-off frequency. In the second case (alias-free), however, the estimated lag values lie alternately on the true curve, the spectrum gives an aliased main peak below and a small peak above the original cut-off frequency.

CONCLUSIONS

The aliasing problem was considered and demonstrated by a simulation example. The Nyquist frequency, the mirror image pattern, the useful frequency range and the folding of higher frequencies were illustrated for the spectrum resulting from the discrete signal processing.

Then, the cubic spline interpolation of the sampled data and its effects on the resulting spectra were studied by simulating random signals with known autocorrelation functions.

The cubic spline interpolation was applied to the sampled signal to obtain a discrete autocorrelation function estimated from the sampled and interpolated values, with a uniform time interval half the sampling interval. The resulting spectrum could be estimated with an apparent cut-off frequency twice the original value. It was observed

that when the original cut-off frequencies were above the positions of the main peaks, the estimated autocorrelations formed good representations of the true functions and could lead to exact spectral estimates; no peaks were observed beyond the original cut-off frequencies and the spectra decayed to zero. On the other hand, small peaks were observed beyond the original cut-off frequencies, for the aliased sampling rates.

The results appear to suggest that, in the uniform sampling, for an alias-free sampling rate, cubic spline interpolation of the sampled signals can yield satisfactory autocorrelation and spectral estimations, with an increased folding frequency and no peaks above the original Nyquist frequency. Conversely, in the case of aliased data, small peaks may appear above the original cut-off frequency extended by the cubic spline interpolation. Such small peaks, that seem to result from the contributions of some points picked up by the cubic spline interpolation (missed in the original aliased data), may indicate the possibility of aliasing being present in the experimentally sampled signal and, for instance, raise the necessity for the data acquisition at a higher rate. Evidently, this can be useful only if the Nyquist frequency, though below, is close to the main peaks and; in other words, if the sampled signal is not too aliased.

APPENDIX

THE CUBIC SPLINE METHOD OF INTERPOLATION

The so-called spline fitting of a curve derives its name from a draftsman's device. A spline is a flexible strip that can be held by weights so that it passes through each of the given points, but goes smoothly from each interval to the next according to the laws of beam flexure. The corresponding mathematical procedure is an adoption of this idea [9].

The cubic spline fit uses a set of cubics passing through the known points, with a new cubic in each interval. To correspond to the idea of the draftsman's spline, it is required that both the slope and the curvature be the same for the pair of cubics joining at each point [9].

Thus, the equations for the cubic spline interpolation (or curve fitting) are derived subject to the above conditions. Consider the i-th interval between the points (x_i, y_i) and (x_{i+1}, y_{i+1}). The equation of the cubic in this interval may be written as:

$$y = a_i(x - x_i)^3 + b_i(x - x_i)^2 + c_i(x - x_i) + d_i \qquad (8)$$

Since it fits at the two end points of the interval, then:

$$y_i = a_i(x_i - x_i)^3 + b_i(x_i - x_i)^2 + c_i(x_i - x_i) + d_i = d_i \qquad (9)$$

and

$$y_{i+1} = a_i(x_{i+1} - x_i) + b_i(x_{i+1} - x_i)^2 + c_i(x_{i+1} - x_i) + d_i = a_i h_i^3 + b_i h_i^2 + c_i h_i + d_i \qquad (10)$$

where

$$h_i = x_{i+1} - x_i \qquad (11)$$

Further, the slopes and curvatures of the joining polynomials have also to be considered. From equation (8), the first and second derivatives may, respectively, be written as:

$$y' = 3a_i(x - x_i)^2 + 2b_i(x - x_i) + c_i \quad (12)$$

$$y'' = 6a_i(x - x_i) + 2b_i \quad (13)$$

Let s_i denote the second derivative at the point (x_i, y_i). Equation (13) then gives:

$$s_i = 6a_i(x_i - x_i) + 2b_i = 2b_i \quad (14)$$

$$s_{i+1} = 6a_i(x_{i+1} - x_i) + 2b_i = 6a_i h_i + 2b_i \quad (15)$$

These equations yield:

$$b_i = s_i / 2 \quad (16)$$

$$a_i = (s_{i+1} - s_i) / 6h_i \quad (17)$$

Substituting for d_i, b_i and a_i from equation (9), (16) and (17), respectively, into equation (10) and solving for c_i gives:

$$c_i = \frac{1}{h_i}(y_{i+1} - y_i) - \frac{h_i}{6}(2s_i + s_{i+1}) \quad (18)$$

Now, the condition that the slopes of the two cubics joining at a point (x_i, y_i) are the same, has to be invoked. Equation (12), for the interval i at $x=x_i$, gives:

$$y'_i = 3a_i(x_i - x_i)^2 + 2b_i(x_i - x_i) + c_i = c_i \quad (19)$$

and for the interval (i-1) at $x=x_i$ (the slope at its right end) yields:

$$y'_i = 3a_{i-1}(x_i - x_{i-1})^2 + 2b_{i-1}(x_i - x_{i-1}) + c_{i-1} \quad (20)$$

$$= 3a_{i-1}h^2_{i-1} + 2b_{i-1}h_{i-1} + c_{i-1}$$

Equating these two expressions, substituting for a_i, b_i, c_i and d_i from equations (17), (16), (18) and (9) respectively, after simplification it leads to:

$$h_{i-1}s_{i-1} + (2h_{i-1} + 2h_i)s_i + h_i s_{i+1} = 6\left(\frac{y_{i+1} - y_i}{h_i} - \frac{y_i - y_{i-1}}{h_{i-1}}\right) \quad (21)$$

Equation (21) applies at each interval, from i=2 to i=n-1, where n is the total number of points. This would yield n-2 equations relating the n values of s_i. Two additional equations, involving s_1 and s_n, may also be obtained by specifying the conditions pertaining to the end intervals of the wholc curve. The suitable approach is to take s_1 as a linear extrapolation from s_2 and s_3, with an analogous linearity relationship for s_n, s_{n-1} and s_{n-2} [9]. This assumption gives:

$$\frac{1}{h_1}(s_2 - s_1) = \frac{1}{h_2}(s_3 - s_2) \Rightarrow h_2 s_1 - (h_1 + h_2)s_2 + h_1 s_3 = 0 \quad (22)$$

$$\frac{1}{h_{n-1}}(s_n - s_{n-1}) = \frac{1}{h_{n-2}}(s_{n-1} - s_{n-2}) \Rightarrow h_{n-1}s_{n-2} - (h_{n-2} + h_{n-1})s_{n-1} + h_{n-2}s_n = o \quad (23)$$

It is convenient to write the set of equations in the matrix form:

$$\begin{bmatrix} h_2 & -(h_1+h_2) & h_1 & 0 & 0 & 0 \\ h_1 & 2(h_1+h_2) & h_2 & 0 & 0 & 0 \\ 0 & h_2 & 2(h_2+h_3) & h_3 & 0 & 0 \\ 0 & 0 & h_3 & 2(h_3+h_4) & h_4 & 0 \\ \vdots & & & & & \\ 0 & \cdots & 0 & h_{n-1} & -(h_{n-2}+h_{n-1}) & 0 \end{bmatrix} \begin{bmatrix} s_1 \\ s_2 \\ s_3 \\ s_4 \\ \vdots \\ s_n \end{bmatrix} = 6 \begin{bmatrix} 0 \\ \frac{y_3 - y_2}{h_2} - \frac{y_2 - y_1}{h_1} \\ \frac{y_4 - y_3}{h_3} - \frac{y_3 - y_2}{h_2} \\ \frac{y_5 - y_4}{h_4} - \frac{y_4 - y_3}{h_3} \\ \vdots \\ 0 \end{bmatrix} \quad (24)$$

If the known points y_i are equally spaced, h_i will be the same and equal to h say, then

a particularly simple matrix equation is obtainable. The vector on the right hand side of equation (24) would, then, have components of $\Delta^2 y$ and the equation reduces to:

$$\begin{bmatrix} 1 & -2 & 1 & 0 & 0 & - & - & - & 0 \\ 1 & 4 & 1 & 0 & 0 & & . & . & 0 \\ 0 & 1 & 4 & 1 & 0 & . & . & . & 0 \\ 0 & 0 & 1 & 4 & 1 & & . & . & 0 \\ M & . & . & & . & . & & . & . \\ 0 & . & . & 0 & 0 & 0 & 1 & 4 & 1 \\ 0 & . & & 0 & 0 & 0 & 1 & -2 & 1 \end{bmatrix} \begin{bmatrix} s_1 \\ s_2 \\ s_3 \\ s_4 \\ M \\ s_{n-1} \\ s_n \end{bmatrix} = \frac{6}{h^2} \begin{bmatrix} 0 \\ \Delta^2 y_1 \\ \Delta^2 y_2 \\ \Delta^2 y_3 \\ M \\ \Delta^2 y_{n-2} \\ 0 \end{bmatrix} \qquad (25)$$

After the s_i values are computed from the above equations, the coefficients a_i, b_i, c_i and d_i are obtainable from equations (17), (16), (18) and (9), respectively. Substituting these into equation (8), gives y corresponding to x in the i-th interval [9].

REFERENCES

[2] Bendat, J. S. and Piersol, A.G., *Random data: analysis and measurement procedures*, Wiley-Interscience, 1986.

[16] Burrus, C. S., et al., *Computer based exercises for signal processing using MATLAB*, Prentice-Hall, 1994.

[11] Chen, M. C., *Biomedical data interpolation for 3-D visualization*, Thesis, Air Force Inst. of Tech., Oh., U.S.A., 1995.

[8] Citriniti, J. H., et al., *Long hot wires and the measurement of large scale turbulent fluctuations*, Proceedings of the 1994 ASME Fluids Eng. Division Summer Meeting (NY, USA), American Soc. of Mechanical Engineering, 183, 1994, pp. 45-52.

[12] Gavrila, D. M., *Hermit deformable contours*, Technical Report, Computer Vision Lab., Maryland University, 1996, pp. 1-18.

[9] Gerald, C. F., *Applied numerical analysis*, Addison-Wesley Publishers, 1970.

[1] Jones, R. H. and Steele, N., *Mathematics in communication theory*, Ellis Horwood Publishers, 1989.

[14] Lane, E. J., *Fitting data using piecewise G1 cubic bezier curves*, Thesis, Naval Postgraduate School, Monterey, CA., U.S.A., 1995.

[10] Madych, W. and Grochenig, K., *Multivariate wavelet representations and approximations*, Technical Report, Dept. of Mathematics, Connecticut University, 1994, pp. 1-84.

[3] Maidanik, G. and Becker, K. J., *Phenomena of aliasing and pass and stop bands in the drive in lieu of ribs on cylindrical shells*, Naval Surface Warfare Center Carderock Div., Bethesda, MD, USA, 1996, pp. 1-195.

[6] Patti, A. J., et al., *Digital video standards conversion in the presence of accelerated motion*, Journal of Signal Processing: Image Communication, 6, 3, 1994, pp. 213-227.

[7] Sommerfeldt, S. D. and Scott, B. L., *Estimating acoustic radiation using wave number sensors*, Proceedings of the 1994 National Conference on Noise Control Engineering (FL, USA), Inst. of Noise Control Eng., 1994, pp. 279-284.

[15] Taha, H. A. *Simulation modeling and simnet*, Prentice-Hall, 1988.

[5] Ten Voorde, B. J., et al., *Spectra of data sampled at frequency-modulated rates in application to cardiovascular signals; part 2: evaluation of fourier transform algorithms*, Journal of Medical & Biological Engineering & Computing, 32, 1, 1994, pp. 71-76.

[13] Unser, M. and Eden, M., *FIR approximation of inverse filters and reconstruction of filter banks*, Journal of Signal Processing, 36, 2, 1994, pp. 163-74.

[4] Varshney, P. K., et al., *Radar signal detection and estimation using time-frequency distributions*, Research Report, Dept. of Electrical and Computer Engineering, Syracuse University, 1995, pp. 1-206.